Superoxide oxidase and reductase activity of cytochrome b559 in Photosystem II

ARTICLE *in* BIOCHIMICA ET BIOPHYSICA ACTA · APRIL 2009

Impact Factor: 4.66 · DOI: 10.1016/j.bbabio.2009.03.017 · Source: PubMed

2 AUTHORS:

Arjun Tiwari
University of Turku
11 PUBLICATIONS **174** CITATIONS
SEE PROFILE

Pavel Pospíšil
Palacký University of Olomouc
58 PUBLICATIONS **1,092** CITATIONS
SEE PROFILE

Biochimica et Biophysica Acta 1787 (2009) 985–994

Contents lists available at ScienceDirect

Biochimica et Biophysica Acta

journal homepage: www.elsevier.com/locate/bbabio

Superoxide oxidase and reductase activity of cytochrome b_{559} in photosystem II

Arjun Tiwari, Pavel Pospíšil *

Department of Experimental Physics, Laboratory of Biophysics, Faculty of Science, Palacký University, tř. Svobody 26, 771 46 Olomouc, Czech Republic

ARTICLE INFO

Article history:
Received 16 December 2008
Received in revised form 19 March 2009
Accepted 26 March 2009
Available online 5 April 2009

Keywords:
Cytochrome b_{559}
Heme iron
Photosystem II
Superoxide oxidase
Superoxide reductase
Superoxide scavenger
Tris-treated PSII membrane

ABSTRACT

This study provides evidence for the superoxide oxidase and the superoxide reductase activity of cytochrome b_{559} (cyt b_{559}) in PSII. It is reported that in Tris-treated PSII membranes upon illumination, both the intermediate potential (IP) and the reduced high potential (HP^{red}) forms of cyt b_{559} exhibit superoxide scavenging activity and interconversion between IP and HP^{red} form. When Tris-treated PSII membranes were illuminated in the presence of spin trap EMPO, the formation of superoxide anion radical ($O_2^{\cdot -}$) was observed, as confirmed by EPR spin-trapping spectroscopy. The observations that the addition of enzymatic (superoxide dismutase) and non-enzymatic (cytochrome *c*, α-tocopherol and Trolox) $O_2^{\cdot -}$ scavengers prevented the light-induced conversion of IP ↔ HP^{red} cyt b_{559} confirmed that IP and HP^{red} cyt b_{559} are reduced and oxidized by $O_2^{\cdot -}$, respectively. Redox changes in cyt b_{559} by an exogenous source of $O_2^{\cdot -}$ reconfirmed the superoxide oxidase and reductase activity of cyt b_{559}. Furthermore, the light-induced conversion of IP to HP^{red} form of cyt b_{559} was completely inhibited at pH>8 and by chemical modification of the imidazole ring of histidine residues using diethyl pyrocarbonate. We proposed that a change in the environment around the heme iron, induced by the protonation and deprotonation of His^{22} residue generates a favorable condition for the oxidation and reduction of $O_2^{\cdot -}$, respectively.

1. Introduction

Cytochrome b_{559} (cyt b_{559}) is an intrinsic and essential component of PSII in all oxygenic photosynthetic organisms [1,2]. It has been shown that cyt b_{559} is a heme-bridged protein heterodimer that consists of α and β subunits encoded by *psbE* and *psbF* genes, respectively [3,4]. The three dimensional structure of PSII from thermophilic cyanobacteria *Thermosynechococcus elongatus* and *Theromosynechococcus vulcanus* showed that α and β subunits are located near to the D2 protein with the heme posed near to the stromal edge of the membrane and perpendicular to the membrane plane [5–8]. As the fifth and sixth axial ligands of the heme iron have been coordinated two histidine residues, His^{22} of the α and His^{17} of the β subunits of the heterodimer [3,9].

The characteristic properties of cyt b_{559} is an appearance of cyt b_{559} in several different redox potential forms spread over the redox potential range from 400 mV to 0 mV [2]. These are high potential (HP) (the midpoint redox potential *E*m ~ +400 mV), the intermediate potential (IP) (*E*m ~ +170 mV), the low potential (LP) (*E*m ~ +60 mV) and the very low potential (VLP) (*E*m ~ 0 mV) forms of cyt b_{559} [10–15]. The conversion of HP to LP form of cyt b_{559} was demonstrated by treatments such as low and high pH treatment [11,16], high concentration of detergent [11,17], uncouplers [16,18], herbicides [18,19], mild heating [20] or ageing [16]. Whereas the conversion of HP to LP form of cyt b_{559} has been widely studied in the past, the reverse conversion of LP to HP forms of cyt b_{559} is poorly understood. It has been presented that LP to HP forms of cyt b_{559} is achieved by the incorporation of purified LP forms of cyt b_{559} into the liposomes [21]. Mizusawa et al. have demonstrated that in the presence of artificial electron donor, the illumination of Tris-treated PSII membranes resulted in the restoration of HP cyt b_{559} [12]. Gadjieva et al. [22] demonstrated that the removal of molecular oxygen from Tris-treated PSII membranes caused the reversible transition between LP and HP form of cyt b_{559}. The authors proposed that molecular oxygen attacks the hydrogen bond between the imidazole ring of histidine and carbonyl group of the polypeptide backbone. More detail explanation of this phenomenon based on potentiometric redox titration has established that it is not LP form rather IP form that is converted to HP form by illumination [12] and anaerobiosis [23].

Although the functional aspect of cyt b_{559} has been extensively worked out during the last three decade, the exact function of this heme protein is still unknown. The largest focus has been given on the involvement of cyt b_{559} in the cyclic electron transport around PSII as a

Abbreviations: Chl, chlorophyll; Cyt b_{559}, Cytochrome b_{559}; DEPC, diethyl pyrocarbonate; EDC, 1-ethyl-3-(3-(dimethylamino)propyl) carbodiimide; *E*m, midpoint redox potential; EMPO, 2-ethoxycarbonyl-2-methyl-3:4-dihydro-2H-pyrrole-1-oxide; EPR, electron paramagnetic resonance; $HO_2^{\cdot}$, hydroperoxyl radical; HP, high potential; IP, intermediate potential form; LP, low potential; PSII, photosystem II; PQH_2, plastoquinol; Q_A, primary quinone electron acceptor in PSII; Q_B, secondary quinone electron acceptor in PSII; ROS, reactive oxygen species; SOD, superoxide dismutase; SOO, superoxide oxidase; SOR, superoxide reductase; Trolox, (±)-6-Hydroxy-2:5:7:8-tetramethylchromane-2-carboxylic acid

* Corresponding author. Tel.: +420 585634164; fax: +420 585225737.
E-mail address: pospip@prfnw.upol.cz (P. Pospíšil).

0005-2728/$ – see front matter © 2009 Elsevier B.V. All rights reserved.
doi:10.1016/j.bbabio.2009.03.017

protective mechanism during the process of photoinhibition [1,24]. It has been proposed that LP^{ox} cyt b_{559} can accept electron from the reduced pheophytin or plastoquinol and thus prevent the over reduction of PSII electron acceptor side, while, HP^{red} form protects against donor side photoinhibition [25–27]. Barber and De Las Rivas [26] have proposed a dual model, which describes the mechanism of interconversion between LP^{ox} and HP^{red} forms during the acceptor and the donor side photoinhibition. Plastoquinone molecule bound at Q_c binding site [18,28] was proposed to maintain the electron transport between pheophytin and heme iron [28,29]. On the opposite site, it has been proposed that HP^{red} cyt b_{559} is oxidized by $P680^+$ with carotenoids and chlorophyll z via a sequential or branched pathway [30–32]. Evidence has been given that cyt b_{559} can provide a plastoquinol oxidase [33,34] and also intrinsic superoxide dismutase activity (SOD) [33,35]. An intrinsic SOD of cyt b_{559} has been previously assigned to either HP or LP form of cyt b_{559} [33,35]. Ananyev et al. [35] demonstrated that the dark reduction of HP cyt b_{559} observed after photoreduction of HP cyt b_{559} is likely caused by $O_2^{\cdot -}$ generated on PSII electron acceptor side. It has been shown that the dark reduction of HP cyt b_{559} was prevented under anaerobic conditions and by heme-active ligand TCNE. Based on the observation that LP cyt b_{559} is reduced by $O_2^{\cdot -}$ generated by xanthine/xanthine oxidase system, Kruk and Strzalka [33] proposed that LP cyt b_{559} exhibits intrinsic SOD activity. The authors demonstrated that the reduction of LP cyt b_{559} is prevented by removal of molecular oxygen or exogenous SOD.

In biological systems, $O_2^{\cdot -}$ is scavenged by SOD which catalyzes dismutation of $O_2^{\cdot -}$ into molecular oxygen and hydrogen peroxide. Reaction mechanism of SOD is based on the reduction and oxidation of the metal center acting as a superoxide oxidase (SOO) and superoxide reductase (SOR), respectively. The discovery of a non-heme iron SOR provided a new insight about how $O_2^{\cdot -}$ is eliminated in anaerobic organisms without the formation of toxic molecular oxygen for them [36–38]. After this, spectroscopic and crystallographic details were reported by several workers for various 1Fe-SOR [39,40] and 2Fe-SOR [37,41]. However, the few reports are available about the interaction of heme iron with $O_2^{\cdot -}$. The most studies were focused on oxidation of $O_2^{\cdot -}$ by ferric heme iron [33,35]. We could not find any literature, which studied the interaction of ferrous heme iron with $O_2^{\cdot -}$.

The current study provides a new insight into $O_2^{\cdot -}$ scavenging activity of ferric and ferrous heme iron of cyt b_{559} in Tris-treated PSII membranes. We present here compelling evidence that $O_2^{\cdot -}$ is involved both in the photoconversion of IP to HP^{red} cyt b_{559} and the reverse photoconversion of HP^{red} to IP cyt b_{559}. Thus, due to these changes during the SOD reaction it is proposed that cyt b_{559} mimics SOO and SOR functions. The either of the two contrasting phenomenons are selected by the redox state of the heme iron and the environment around the imidazole ring *i.e.* reduced/oxidized and protonated/deprotonated state, respectively. Our model provides the mechanistic aspects of both the reactions based on the analogy with the outer-sphere oxidation of $O_2^{\cdot -}$ (SOO activity) and the inner-sphere reduction of $HO_2^{\cdot}$ (SOR activity).

2. Materials and methods

2.1. PSII membranes preparation

PSII membranes from spinach were prepared using the method of Berthold et al. [42] with the modifications described in Ford and Evans [43]. PSII membranes were resuspended in a medium containing 400 mM sucrose, 10 mM NaCl, 5 mM $CaCl_2$ and 40 mM Mes–NaOH (pH 6.5) and stored at −80 °C. Tris-treated PSII membranes were prepared by incubation of PSII membranes (1 mg Chl ml^{-1}) in a buffer containing 0.8 M Tris–HCl (pH 8) for 30 min at 4 °C, in the darkness with continuous gentle stirring. After treatment, PSII membranes were washed twice in 400 mM sucrose, 10 mM NaCl, and 5 mM $CaCl_2$ and 40 mM Mes–NaOH (pH 6.5). The oxygen evolution activity in Tris-treated membranes measured with Clark-type oxygen electrode (HANSATECH, UK) was completely suppressed compared to control PSII membranes. PSII activity as the electron transfer rate from DPC to DCPIC was 300 μM of $DCPIPH_2$ mg^{-1} Chl h^{-1}. In some measurements, 500 U ml^{-1} superoxide dismutase (EC 1.15.1.1, from Bovine liver) (Sigma), 400 μM cytochrome *c* (from Bovine heart) (Sigma), 250 μM α-tocopherol (Aldrich) and 250 μM Trolox (a water-soluble analogue of α-tocopherol) (Fluka) were added to the sample before or after illumination, as indicated in the text.

2.2. Modification treatment

Chemical modification of carboxyl groups was performed using 1-ethyl-3-(3-(dimethylamino)propyl) carbodiimide (EDC) (Aldrich) as described in [44]. PSII membranes (250 μg Chl ml^{-1}) were treated with 5 mM EDC (Chl:EDC ratio was 1:4 (w/w)) in 50 mM Mes– NaOH (pH 6.5), 15 mM NaCl, 5 mM $MgCl_2$ and 400 mM sucrose for 30 min on ice under continuous stirring in the dark. The reaction was terminated by the addition of a large volume of buffer solution after the incubation period and was centrifuged immediately, followed by two washing steps in the same solution.

Imidazole rings of the histidine residues were modified using diethyl pyrocarbonate (DEPC) (Aldrich) according to the method of Hegde et al. [45] with modification described in Roncel et al. [15]. PSII membranes (50 μg Chl ml^{-1}) were treated with 5 mM DEPC for 15 min at 25 °C under stirring. After incubation, concentrated histidine solution was added to PSII membranes to the final concentration of 20 mM and incubated for 1 min in the dark. PSII membranes were twice washed and suspended in 50 mM Mes– NaOH (pH 5.5).

2.3. Optical measurements

Redox properties of cyt b_{559} were monitored by following the absorbance changes using Olis RSM 1000 spectrometer (Olis Inc., Bogart, Georgia, USA). Tris-treated PSII membranes (100 μg Chl ml^{-1}) were treated in a 3 ml quartz cuvette at 20 °C using 50 μM potassium ferricyanide (reference cuvette), 8 mM hydroquinone (test cuvette) and 5 mM sodium ascorbate (test cuvette). Each step was followed by dark adaptation for 5 min with a continuous slow stirring inside the spectrophotometer using a tiny bar magnet unless stated otherwise. After switching off the stirring, absorption spectra were recorded from 530 nm to 580 nm. The spectrum slit width was 0.12 μm, the total band pass 0.5 nm and the scan speed 50 nm per min. The amount of different states of cyt b_{559} was calculated from the average spectra of five measurements. Different forms of cyt b_{559} were determined by treatment minus control spectrum. Total HP form was determined by difference spectra of hydroquinone-reduced minus ferricyanide-oxidized cyt b_{559}. The IP form was determined by difference spectra of ascorbate-reduced minus hydroquinone-reduced cyt b_{559}. The photo-induced HP^{red} form was determined by difference spectra of illuminated (100 and 300 s) minus ferricyanide-oxidized dark-adapted cyt b_{559}. It was observed that addition of hydroquinone in illuminated samples did not bring about further changes in peak intensities of HP and IP forms. Therefore, it is concluded that light-induced peak was of HP^{red} form. Thus, it could be replaced for calculations with hydroquinone-reduced spectra for the measurements of HP form as “light minus ferricyanide spectra” and for the measurements of IP form as “ascorbate minus light spectra” in illuminated samples. We carried out several measurements in illuminated samples by putting hydroquinone as an additional step and HP/IP forms were calculated by using hydroquinone-reduced spectra but it was just an additional step and did not make any difference in the results and main finding of this work. Thus, the additional step of using hydroquinone in illuminated samples was excluded from the further experiments. Illumination was performed at 1000 μmol photons m^{-2} s^{-1} intensity by 90° rotating the cuvette at each 15 s

interval using continuous illumination by halogen cold light source (Schott KL 1500, Schott AG, Mainz, Germany).

2.4. Potentiometric measurements

Potentiometric redox titrations were performed according to the methods of Dutton [46] with some modifications described in Roncel et al. [15]. Redox potentials were measured using potentiometer Oxi 340i (*WTW GmbH*, Weilheim, Germany) provided with Pt–Ag/AgCl redox microelectrode (Pt 5900 A, Schott Instruments GmbH, Mainz, Germany) simultaneously with absorbance changes at 559 nm. Redox microelectrode (diameter of 5 mm) was immersed in the test cuvette inside of the spectrophotometer in such a way so that it does not affect the light path. Prior to the measurements, samples were bubbled with argon and measurements were performed under argon environment at room temperature. Reductive potentiometric titrations were performed under aerobic conditions in Tris-treated PSII membranes (100 μg Chl ml^{-1}) previously oxidized with 2 mM potassium ferricyanide ($Em = 430$ mV, pH 7). In addition to potassium ferricyanide, the following mediators were used: 20 μM p-benzoquinone ($Em = +280$ mV, pH 7), 20 μM 2,5-dimethyl-p-benzoquinone ($Em = +180$ mV, pH 7), 20 μM N-methylphenazonium methosulfate ($Em = +80$ mV, pH 7), 20 μM sodium ascorbate ($Em = +60$ mV, pH 7), 20 μM sodium dithionite ($Em = -660$ mV, pH 7). The stirring was switched on before the addition of mediators and switched off before measurements as described above. The dilution resulting from the titration was compensated by the addition of buffer solution in the reference cuvette. Midpoint redox potential and fraction of reduced cyt b_{559} were determined by the fitting of the redox titration curve to Nernst equation in accordance with one-electron process ($n = 1$) for one or two components.

2.5. EPR spin-trapping spectroscopy

The spin-trapping was accomplished by EMPO, 5-(ethoxycarbonyl)-5-methyl-1-pyrroline N-oxide (Alexis Biochemicals, Lausen, Switzerland). Tris-treated PSII membranes (150 μg Chl ml^{-1}) were illuminated in a glass capillary tube (Blaubrand® intraMARK, Brand, Germany) in the presence of 25 mM EMPO, 100 μM desferal, 40 mM Mes– NaOH (pH 6.5). Illumination was performed with continuous white light (1000 μmol photons m^{-2} s^{-1}) using a halogen lamp with a light guide (KL 1500 electronic, Schott, Germany) and spectra were recorded using EPR spectrometer MiniScope MS200 (Magnettech GmbH, Germany). Signal intensity was evaluated as a relative height of the central doublet of the first derivate of the absorption spectrum. EPR conditions were as follows: microwave power, 10 mW; modulation amplitude, 1 G; modulation frequency, 100 kHz; sweep width, 100 G; scan rate, 1.62 G s^{-1}. Superoxide was generated from 1 mM potassium superoxide (KO_2) (Fluka) in dry dimethyl sulfoxide (DMSO). KO_2 powder was dissolved into dry DMSO previously bubbled with argon gas. To promote dissolution of KO_2 1 mM crown ether 18-C-6 (Aldrich) was used in DMSO.

3. Results

3.1. Reversible photoconversion of IP ↔ HP^{red} cyt b_{559} in Tris-treated PSII membranes

Light-induced redox state and redox potential changes of cyt b_{559} were investigated in Tris-treated PSII membranes by measuring the absorption changes at 559 nm. In Tris-treated PSII membranes, cyt b_{559} was found in ascorbate-reducible IP form, whereas hydroquinone-reducible HP form was rather absent (Fig. 1A, left column). Reductive potentiometric titrations performed under complete anaerobic condition in Tris-treated PSII membranes which were previously oxidized with ferricyanide showed the existence of two components

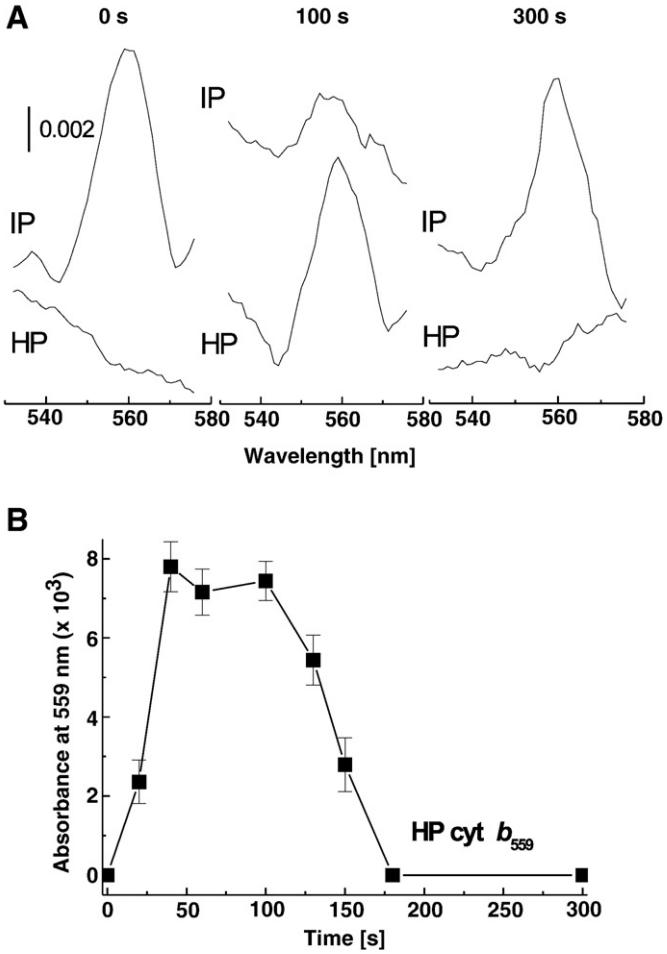

Fig. 1. Light-induced redox changes of cyt b_{559}. (A) Redox difference spectra of cyt b_{559} measured in dark and after illumination in Tris-treated PSII membranes. The samples (100 μg Chl ml^{-1}) were illuminated using white light (1000 μmol photons m^{-2} s^{-1}) for the period indicated in the Fig. In the left column, HP and IP spectra represent the hydroquinone minus ferricyanide and ascorbate minus hydroquinone absorbance spectra, respectively. In the middle and right column, HP spectra show the light minus ferricyanide-oxidized spectra, whereas spectra of IP form represent ascorbate minus light spectra. The spectra were smoothed by using five points averaging of spectra using the Origin v4.1 software. (B) Time profile of formation of HP cyt b_{559} by illumination in Tris-treated PSII membranes. The intensity of the absorption signal was calculated as the height of peak at 559 nm from a reference line connecting the lowest points near 545 and 575 nm. Each data point represents the mean value of at least three measurements ± SD.

with the midpoint redox potential $Em \sim +300$ mV and $+125$ mV (Fig. 2A). It was demonstrated previously that removal of molecular oxygen converts ascorbate-reducible forms (LP/IP) into hydroquinone-reducible form (HP) [22,23]. Thus, measurement of the redox potential shift due to illumination in PSII membranes was only possible in the presence of molecular oxygen. Although it may cause a downshift of redox potential in the region of IP and LP form yet any interference of molecular oxygen in the range of HP form is not reported. Therefore, further titrations have been carried out in treated samples in aerobic condition so as to any shift in redox potential from IP to HP form due to illumination could be identified. Due to the interference of molecular oxygen, reoxidation of LP form occurs below 100 mV ambient redox potential thus complete oxidation could not be achieved. Therefore, in aerobic titrations data points of the titration have been considered only above 100 mV. When Tris-treated PSII membranes were illuminated for 100 s, HP^{red} form was observed, whereas the content of IP cyt b_{559} significantly decreased (Fig. 1A, middle column). Potentiometric titrations performed in Tris-treated PSII membranes illuminated for 100 s showed the existence of a component with

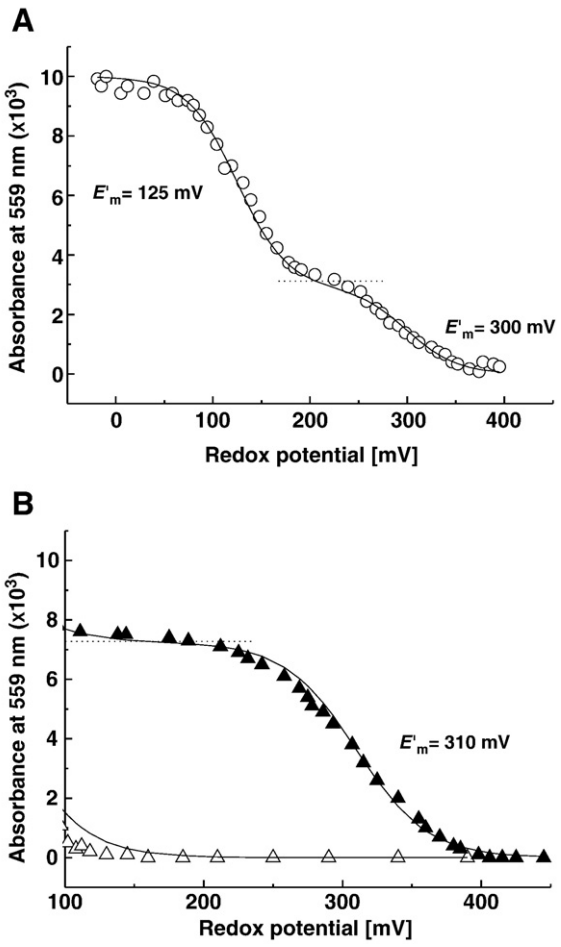

Fig. 2. Reductive potentiometric titrations of cyt b_{559}. (A) Tris-treated PSII membranes (100 μg Chl ml^{-1}) in complete anaerobic environment, (B) Tris-treated PSII membranes (100 μg Chl ml^{-1}) titrated in air after short bubbling of argon after illumination with white light (1000 μmol photons m^{-2} s^{-1}) for (▲), 100 s and (△), 300 s. The symbols show data points of the titration curve, whereas solid lines represent the best fits of the experimental data to Nernst equation in accordance with the one-electron process ($n=1$) for one (A) or two (B) components. Dotted line represents the cross-over between two redox components obtained by the fitting procedure.

*E*m ~ + 310 mV (Fig. 2B). These results indicate that illumination of Tris-treated PSII membranes caused conversion of IP cyt b_{559} (*E*m ~ + 125 mV) to HP^{red} cyt b_{559} (*E*m ~ + 310 mV). When Tris-treated PSII membranes were exposed to more prolonged illumination for 300 s, HP^{red} form was completely suppressed, whereas the content of IP cyt b_{559} was re-established (Fig. 1A, right column). Potentiometric titrations performed in Tris-treated PSII membranes, which were illuminated for 300 s, did not show any component with *E*m value in the range of HP form (Fig. 2B). Relative content of HP^{red} cyt b_{559} as a function of illumination time is shown in Fig. 1B. It is clearly seen that 1) IP form was converted into HP^{red} form within 40 s of continuous illumination, 2) reoxidation of cyt b_{559} occurred for more than 100 s of continuous illumination and 3) cyt b_{559} was completely oxidized within 180 s and remained oxidized even after further illumination. These observations showed that illumination of Tris-treated PSII membranes results in the reversible photoconversion of IP ↔ HP^{red} cyt b_{559}.

3.2. Photogeneration of ROS in Tris-treated PSII membranes

To study the production of reactive oxygen species (ROS) in Tris-treated PSII membranes, EPR spin-trapping technique was used. The spin-trapping was accomplished in the presence of the spin trap compound EMPO which is known to react either with superoxide anion ($O_2^{\cdot -}$) or hydroxyl ($^{\cdot}OH$) radical forming the spin trap-superoxide (EMPO–OOH) or the spin trap-hydroxyl (EMPO–OH) adduct, respectively [47,48]. Addition of EMPO to Tris-treated PSII membranes in the dark resulted in the formation of neither EMPO–OOH nor EMPO–OH adduct EPR signals (Fig. 3A). When Tris-treated PSII membranes were illuminated in the presence of EMPO, EPR spectra were detected that exhibit the peaks and hyperfine splitting characteristics of EMPO–OOH adduct (Fig. 3A). Fig. 3B shows the time profile of EMPO–OOH adduct generation measured up to 300 s illumination. No EMPO–OOH adduct EPR signal was observed when the buffered solution of pure EMPO spin trap was illuminated. This indicates that PSII membranes are required for the appearance of EMPO–OOH adduct (data not shown). The observation that EMPO–OOH adduct EPR signal is formed upon illumination reveals that $O_2^{\cdot -}$ is produced in Tris-treated PSII membranes.

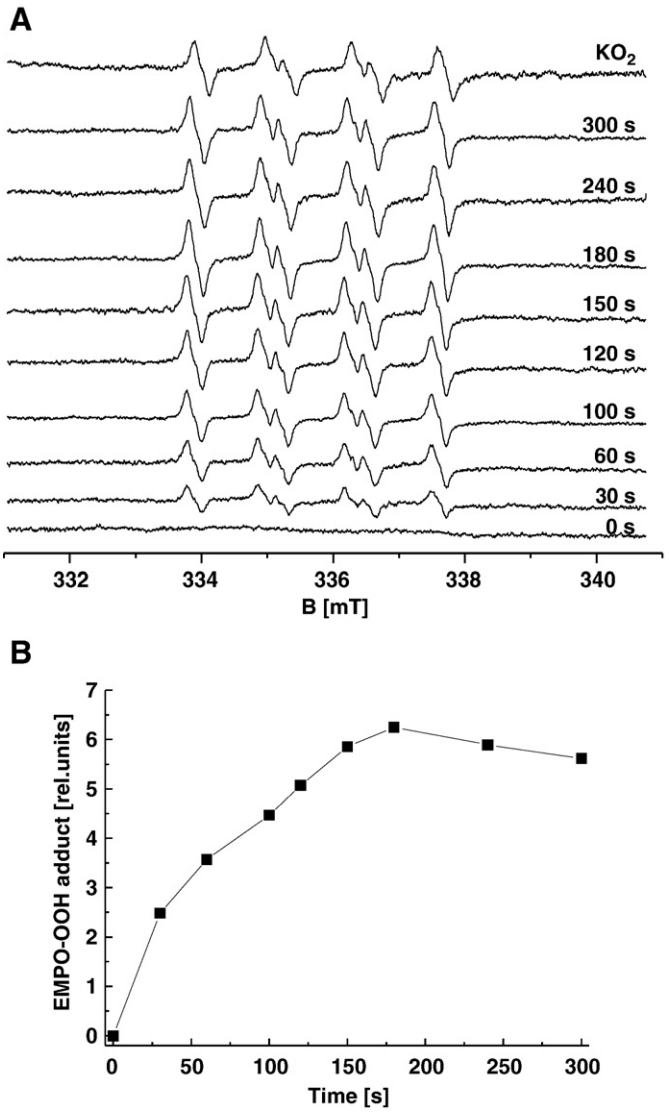

Fig. 3. Detection of superoxide using EPR spin-trapping spectroscopy. (A) Light-induced EPR spin-trapping spectra of the EMPO–OOH adduct measured in Tris-treated PSII membranes after illumination for the time period indicated in the figure. Spectra were obtained after the illumination of the sample (150 μg Chl ml^{-1}) with white light (1000 μmol photons m^{-2} s^{-1}) in the presence of 25 mM EMPO, 100 μM desferal and 40 mM MES– NaOH (pH 6.5). The upmost trace labeled KO_2 shows the EPR signal of the EMPO–OOH adduct generated by 1 mM potassium superoxide in dry DMSO. EPR spectra were plotted as the first derivative of the EPR absorption. (B) Time profile of the formation of the EMPO–OOH adduct EPR signal in Tris-treated PSII membranes. The intensity of EPR signal was evaluated as the relative height of the central doublet of the first derivative of the EPR absorption spectrum.

3.3. Effect of ROS scavengers on reversible photoconversion of IP ↔ HP^{red} cyt b_{559}

To test an involvement of ROS in the reversible photoconversion of IP ↔ HP^{red} cyt b_{559}, the effect of $O_2^{\cdot -}$ and H_2O_2 scavengers on the redox properties of cyt b_{559} was tested. When enzymatic (SOD) or non-enzymatic (cytochrome *c*, α-tocopherol and Trolox) $O_2^{\cdot -}$ scavengers were added to Tris-treated PSII membranes prior to the illumination, IP to HP^{red} conversion of cyt b_{559} was prevented (Fig. 4A). Fig. 4C shows that SOD and cytochrome *c* completely suppressed the light-induced generation of $O_2^{\cdot -}$. It was observed that α-tocopherol and Trolox interacted with EMPO–OOH adduct in the dark, however, SOD and cytochrome *c* did not show any such effects.

In order to test the effect of $O_2^{\cdot -}$ scavengers on light-induced conversion of cyt b_{559} from HP^{red} to IP form, HP^{red} cyt b_{559} was firstly generated by pre-illumination of Tris-treated PSII membranes for 100 s followed by addition of $O_2^{\cdot -}$ scavengers and re-illumination for 200 s. It was observed that in the presence of $O_2^{\cdot -}$ scavengers, the reverse conversion from HP^{red} to IP form of cyt b_{559} was prevented (Fig. 4B). Fig. 4D demonstrates the effect of $O_2^{\cdot -}$ scavengers on formation of EMPO–OOH adduct signal upon re-illumination. The EMPO spin trap and $O_2^{\cdot -}$ scavengers were added in 100 s pre-illuminated PSII membranes prior to re-illumination (Fig. 4D).

Addition of catalase to Tris-treated PSII membranes prior to the illumination has no effect on IP to HP^{red} conversion of cyt b_{559} (Fig. 5A, left column). Similarly, when HP^{red} cyt b_{559} was firstly generated by 100 s pre-illumination of Tris-treated PSII membranes and further catalase was added to prevent H_2O_2 formation, no effect of catalase on conversion of HP^{red} to IP cyt b_{559} was observed during re-illumination (Fig. 5A, right column). These results reveal that the participation of H_2O_2 in these reactions is unlikely, whereas it has been confirmed that the reversible photoconversion of IP ↔ HP^{red} forms is a result of $O_2^{\cdot -}$ scavenger function of cyt b_{559}.

3.4. Effect of exogenous source of superoxide on redox changes of cyt b_{559}

To test the involvement of $O_2^{\cdot -}$ in photoconversion of IP ↔ HP^{red} cyt b_{559}, the effect of exogenous source of $O_2^{\cdot -}$ on redox changes of cyt b_{559} was studied. When KO_2 in dry DMSO was added to Tris-treated PSII membranes, formation of HP^{red} cyt b_{559} was observed, whereas IP cyt b_{559} was suppressed (Fig. 5B, left column). This reaction was limited by amount of added KO_2 and very short life of KO_2 in aqueous medium. Thus no further transformation of HP^{red} form into IP form was observed. In order to test the effect of exogenously generated $O_2^{\cdot -}$ on HP^{red} cyt b_{559}, HP^{red} form was first generated by illumination for 100 s and then KO_2 in dry DMSO was mixed in these samples in the dark. As a result of interaction of $O_2^{\cdot -}$ with HP^{red} form, HP^{red} cyt b_{559} was diminished, whereas IP cyt b_{559} was generated which was detected by further addition of sodium ascorbate (Fig. 5B, left column). These results reveal that exogenously generated $O_2^{\cdot -}$ also caused the reversible conversion of IP ↔ HP^{red} cyt b_{559}.

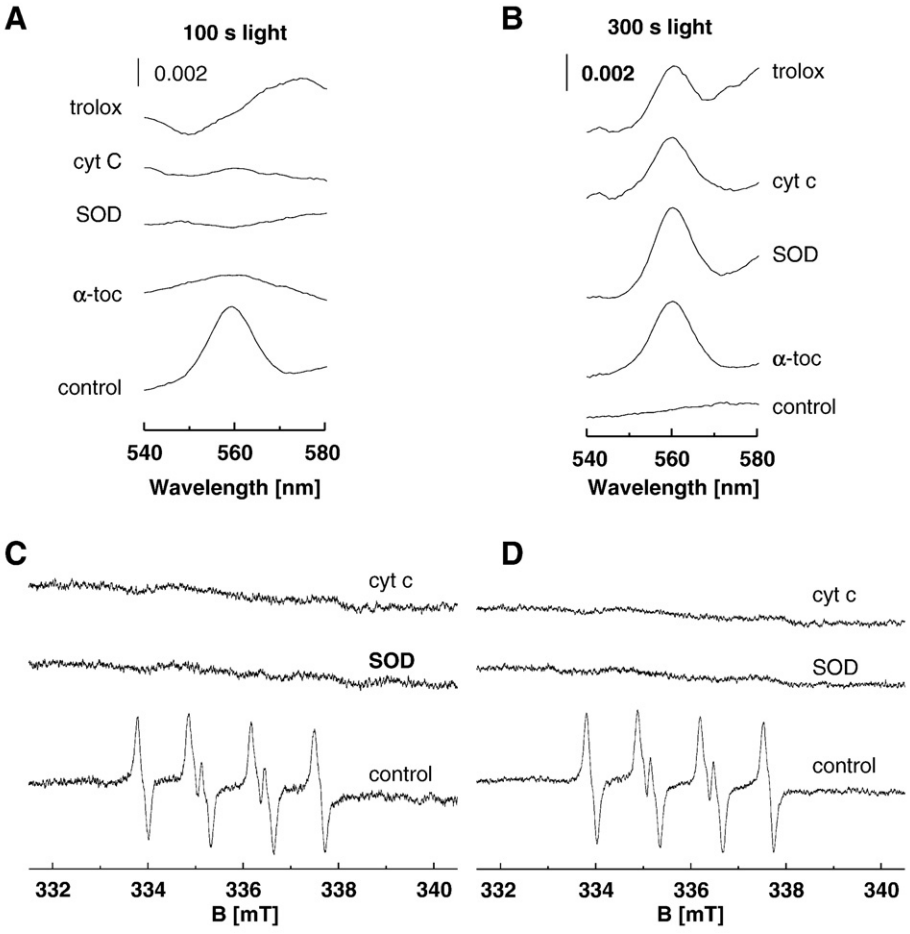

Fig. 4. Effect of superoxide scavengers on the light-induced redox changes of cyt b_{559} and superoxide production. (A, B) Light-induced redox difference spectra of cyt b_{559} in Tris-treated PSII membranes. (C, D) Light-induced EPR spin-trapping spectra of the EMPO–OOH adduct. In A and C, the sample (100 μg Chl ml^{-1}) was illuminated in the presence of the scavengers. In B and D, the sample was firstly illuminated for 100 s in the absence of scavengers to generate HP^{red} cyt b_{559} and after addition of scavengers further illuminated for 200 s. The concentrations of the scavengers were: 500 U ml^{-1} SOD, 400 μM cytochrome *c*, 50 μM α-tocopherol and 250 μM Trolox. In (A, B) and (C, D) other experimental conditions were the same as in Figs. 1A and 3A, respectively.

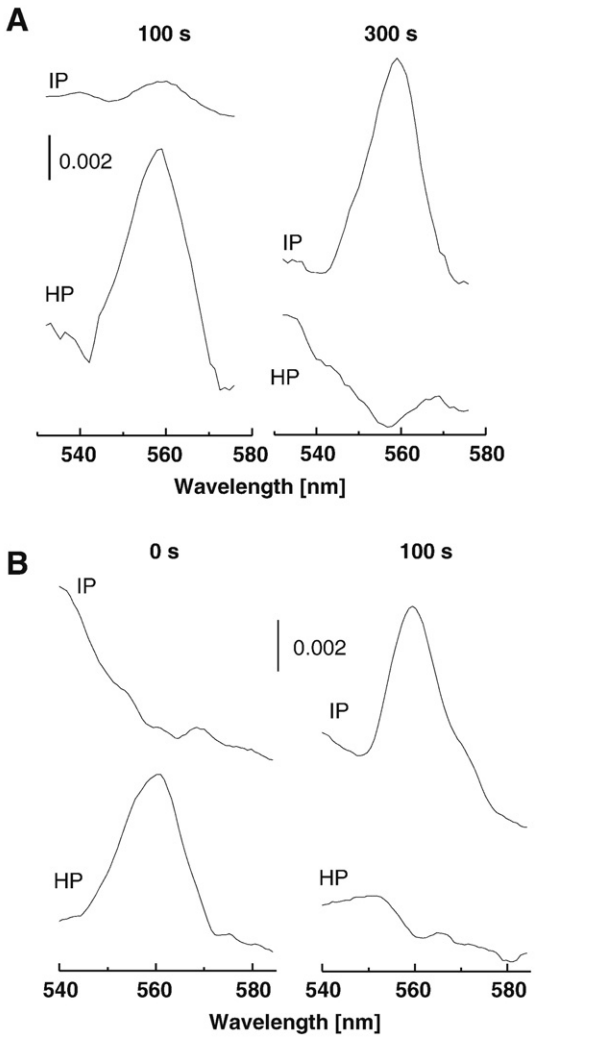

Fig. 5. Redox changes of cyt b_{559} by addition of the catalase and the exogenous source of superoxide in dark and illuminated Tris-treated PSII membranes. (A) In the left column, Tris-treated PSII membranes (100 μg Chl ml^{-1}) were illuminated for 100 s in the presence of 4000 U ml^{-1} catalase. In the right column, the sample (100 μg Chl ml^{-1}) was firstly illuminated for 100 s in the absence of catalase followed by the addition of catalase and further illuminated for 200 s. (B) In the left column, 1 mM KO_2 in dry DMSO was added to Tris-treated PSII membranes (100 μg Chl ml^{-1}) in dark which were having cyt b_{559} in IP form. In the right column, 1 mM KO_2 in dry DMSO was added in 100 s pre-illuminated Tris-treated PSII membranes (100 μg Chl ml^{-1}), which were having cyt b_{559} in HP form. Other experimental conditions were the same as in Fig. 1A.

3.5. Effect of pH on reversible photoconversion of IP ↔ HP^{red} cyt b_{559}

It has been demonstrated that a change in the redox properties of cyt b_{559} is accompanied by formation of the hydrogen bond between the histidine ligand and the polypeptide backbone [14]. More recently, the protonation of amino acid and formation of the hydrogen bond between His^{22} and carbonyl group of α polypeptide was demonstrated as an essential requirement for attaining HP form [15,16,49]. In the light of these facts, we have examined the effect of pH on the light-induced conversion of IP to HP^{red} cyt b_{559} in Tris-treated PSII membranes. As pH was increased above 6.5, the light-induced formation of HP^{red} cyt b_{559} was gradually decreased and completely suppressed above pH 8 (Fig. 6). It can be seen that pH dependence of HP^{red} cyt b_{559} formation is sigmoidal with a $pK_a \sim 7.4$. The observed pK_a value is within the range described for a histidine residue and thus the ionizing group can be assigned to histidine [50]. Based on these considerations it is proposed that the protonation of histidine seems to be involved in the conversion of IP to HP^{red} cyt b_{559}. Therefore, subsequent steps in our investigations were focused on the modification of carboxyl and imidazole group separately in these polypeptides, which might be playing an essential role in the re-establishing of HP^{red} form.

3.6. Effect of EDC and DEPC reversible photoconversion of IP ↔ HP^{red} cyt b_{559}

The main reactive groups responsible for the conversion of IP to HP^{red} cyt b_{559} have been identified by using the selective modification of the carboxyl groups and the imidazole groups in Tris-treated PSII membranes. Participation of carboxyl group in the conversion of IP to HP^{red} cyt b_{559} was investigated using a water-soluble carbodiimide 1-ethyl-3-[(3-dimethylamino)propyl] carbodiimide (EDC), a chemical modifier of free carboxyl group of the amino acid residues. It is known that EDC couples the carboxyl groups to the primary amines, whereas an amine-reactive O-acylisourea is forming as an intermediate [51]. To study the involvement of histidine in the light-induced conversion of IP to HP^{red} cyt b_{559}, diethyl pyrocarbonate (DEPC) was used, which is known to substitute proton at nitrogen on the imidazole ring, whereas the other nitrogen is not affected [45]. Fig. 7A and B show that replacement of proton with either of the modification agents does not affect the dark state of cyt b_{559}. The observation that the light-induced formation of HP^{red} cyt b_{559} was observed in Tris-treated PSII membranes containing the modified carboxyl groups reveals that the involvement of carboxyl group in IP to HP^{red} conversion is unlikely. However, the conversion of IP to HP^{red} cyt b_{559} upon illumination was completely prevented in Tris-treated PSII membranes that contain modified imidazole ring of histidine residues (Fig. 7B). Based on the fact that the modification of imidazole group was performed in Tris-treated PSII membranes, where cyt b_{559} is in the deprotonated IP state, the complete adduct of imidazole-DEPC complex could be formed. Thus, it is evident that the preclusion of protonation of the imidazole group was solely responsible reason for the loss of conversion from IP to HP^{red} form of cyt b_{559}.

4. Discussion

In this study, light-induced redox, redox potential and acid-base properties of cyt b_{559} were studied in PSII membranes depleted of the water-splitting manganese complex by Tris treatment. The results obtained showed that illumination of Tris-treated PSII membranes results in the reversible photoconversion of cyt b_{559} from IP ↔ HP^{red} form comprising of 1) the conversion of IP ($Em \sim +125$ mV) to HP^{red} ($Em \sim +310$ mV) form and 2) the reverse conversion of HP^{red} to IP form (Figs. 1, 2). In accordance with these observations, it has been previously demonstrated that the application of continuous or pulsed

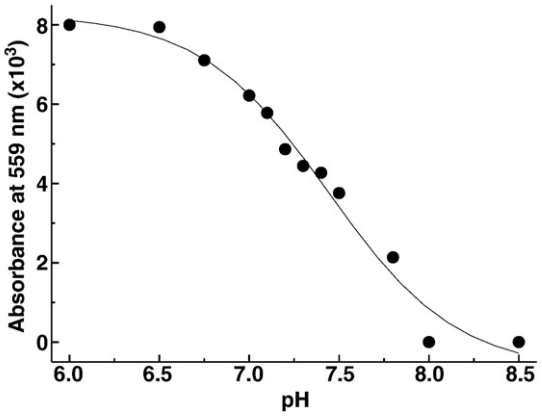

Fig. 6. Effect of pH on the light-induced formation of HP^{red} cyt b_{559}. Tris-treated PSII membranes (100 μg Chl ml^{-1}) were illuminated for 100 s in 40 mM Mes– NaOH (pH 6.5) or 40 mM Hepes (pH 7–8). The pK_a value was determined as pH value corresponding to the half of HP^{red} cyt b_{559}. Other experimental conditions were the same as in Fig. 1B.

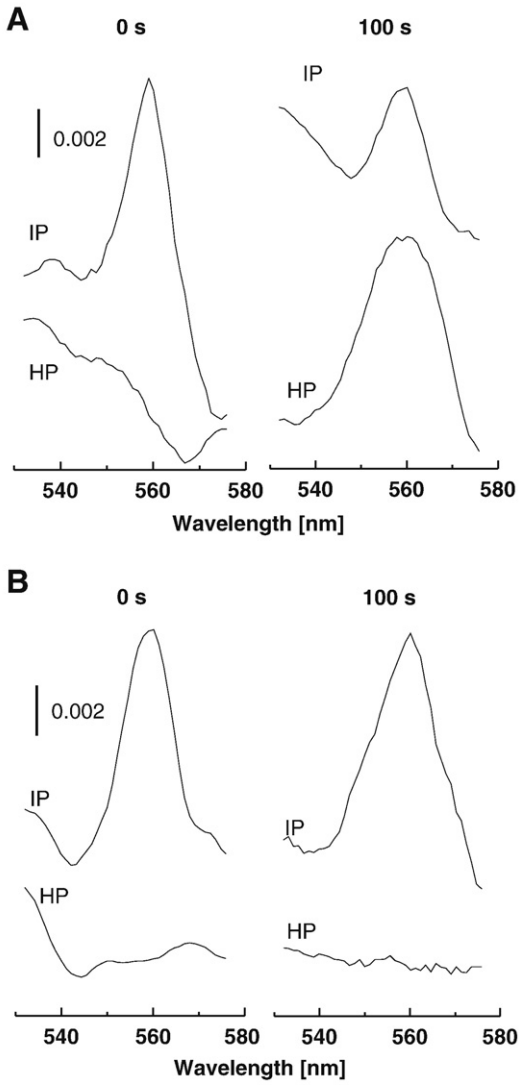

Fig. 7. Redox changes of cyt b_{559} in dark and upon illumination in Tris-treated PSII membranes with modified amino acid. (A) Redox difference spectra of cyt b_{559} measured in dark and after illumination in Tris-treated PSII membranes with modified carboxyl group. Modification of the carboxyl groups was performed using EDC treatment. After modification, the sample (100 μg Chl ml^{-1}) was illuminated for 100 s in 50 mM Mes– NaOH (pH 6.5). (B) Redox difference spectra of cyt b_{559} measured in dark and after illumination in Tris-treated PSII membranes with modified imidazole ring. Modifications of the imidazole ring were performed using DEPC treatment. The sample (100 μg Chl ml^{-1}) was illuminated for 100 s in 50 mM Mes (pH 5.5).

light to Mn-depleted PSII membranes caused the restoration of HP cyt b_{559} [12]. The dual model proposed by Barber and De Las Rivas [26,49], which described pH-dependent interconversion between LP and HP forms with protonation/deprotonation reactions is found to be in good agreement with the current work. We demonstrated $O_2^{\cdot-}$ as a key regulator responsible for the reversible conversion between IP and HP^{red} form of cyt b_{559}.

4.1. Role of superoxide in the photoconversion of $IP \leftrightarrow HP^{red}$ cyt b_{559}

Using EPR spin-trapping technique, we have demonstrated that $O_2^{\cdot-}$ is produced in Tris-treated PSII membranes upon illumination (Fig. 3). Due to the lack of electron donation form water-splitting manganese complex to PSII in Tris-treated PSII membranes, the source of electron to molecular oxygen is likely different from that proposed in fully active PSII membranes [29,34,52]. Based on the observation that $O_2^{\cdot-}$ scavengers prevented IP to HP^{red} conversion of cyt b_{559}, the involvement of $O_2^{\cdot-}$ is substantiated in the conversion of cyt b_{559} from IP to HP^{red} form (Fig. 4). This proposal has been supported by the observation that exogenously generated $O_2^{\cdot-}$ caused conversion of $IP \leftrightarrow HP^{red}$ cyt b_{559} (Fig. 5B). An interaction of $O_2^{\cdot-}$ with ferric heme iron is proposed to result in the formation of ferrous heme iron, whereas O_2 is released as by-product

$$\text{IP cyt } b_{559}(Fe^{3+}) + O_2^{\cdot-} + H^+ \rightarrow \text{HP cyt } b_{559}(Fe^{2+})(H^+) + O_2. \quad \text{(A)}$$

As the midpoint redox potential of the $O_2/O_2^{\cdot-}$ redox couple (pH 7) and Fe^{3+}/Fe^{2+} redox couple in IP form of cyt b_{559} is −160 mV [53] and 125 mV (Fig. 2A), respectively, the reduction of ferric heme iron by $O_2^{\cdot-}$ is favorable from thermodynamic point of view. Similarly, the observation that the reverse conversion of HP^{red} to IP form of cyt b_{559} is suppressed by $O_2^{\cdot-}$ scavengers indicates that $O_2^{\cdot-}$ is involved in the reverse conversion of HP^{red} to IP form of cyt b_{559} (Fig. 4). The fact that exogenously generated $O_2^{\cdot-}$ caused reverse conversion of $HP^{red} \leftrightarrow$ IP cyt b_{559} (Fig. 5B) confirmed the involvement of $O_2^{\cdot-}$ in conversion of $HP^{red} \leftrightarrow$ IP cyt b_{559}. It is proposed that the interaction of protonated form of superoxide $HO_2^{\cdot}$ (hydroperoxyl radical) with ferrous heme iron results in the formation of ferric heme iron and H_2O_2.

$$\text{HP cyt } b_{559}(Fe^{2+})(H^+) + HO_2^{\cdot} \rightarrow \text{IP cyt } b_{559}(Fe^{3+}) + H_2O_2. \quad \text{(B)}$$

The midpoint redox potential of Fe^{3+}/Fe^{2+} redox couple in HP form of cyt b_{559} and midpoint redox potential of the $O_2^{\cdot-}/H_2O_2$ redox couple are 310 mV (Fig. 2B) and 890 mV (pH 7) [53], respectively. Thus, the ferrous heme iron might reduce $O_2^{\cdot-}$ to H_2O_2. It is proposed that interacting species is presumably $HO_2^{\cdot}$ because it carries an additional proton to the heme as well as in this form it can be more easily diffusible inside the membrane.

4.2. Role of protonation of histidine residue in the photoconversion of $IP \leftrightarrow HP^{red}$ cyt b_{559}

The observation that photoconversion of IP to HP^{red} cyt b_{559} is completely suppressed above pH 8 indicates that protonation of amino acid is essential for the formation of HP^{red} cyt b_{559} (Fig. 6). The $pK_a \sim 7.4$ determined from pH dependence of the photoconversion of IP to HP^{red} cyt b_{559} is closed to pK_a value of protonation of the imidazole group. It has been shown that pK_a of the imidazole ring ranges between pH 6 and 8 with a particular value modulated by its environment within the proteins [50]. In accordance with this, it has been previously suggested that in LP^{ox} form of cyt b_{559}, one of the hydrogen bond between imidazole ring of histidine and carbonyl group of polypeptides is absent [14,15]. Based on these suggestions, it has been proposed that the protonation/deprotonation reactions regulate the conversion between the two states of cyt b_{559} [15,16,49].

Selective modification of the imidazole groups using histidine-modifying reagent DEPC showed that imidazole groups of histidine is involved in photoconversion of IP to HP^{red} cyt b_{559}. Thus, it could be concluded that protonation of the axial histidine is an essential requirement for formation of HP form. In accordance with our observation, it has been previously demonstrated that protonation of histidine residue coordinated to the heme might play a crucial role in the determination of redox potential properties of cyt b_{559} [15].

4.3. Superoxide dismutase activity of cyt b_{559}

On the basis of the results presented in this study, a model for SOO and SOR activity of cyt b_{559} is proposed. The model shows a plausible explanation of superoxide-induced conversion of cyt b_{559} from IP to HP^{red} form as well as the reverse conversion of HP^{red} to IP form (Scheme 1). Reaction pathways in the redox active metal of superoxide-scavenger enzymes are assigned by electronic properties of the metal, which is tuned by coordinated ligands and hydrogen bond with nearby amino acid [38,54–56]. It is well known that the redox active

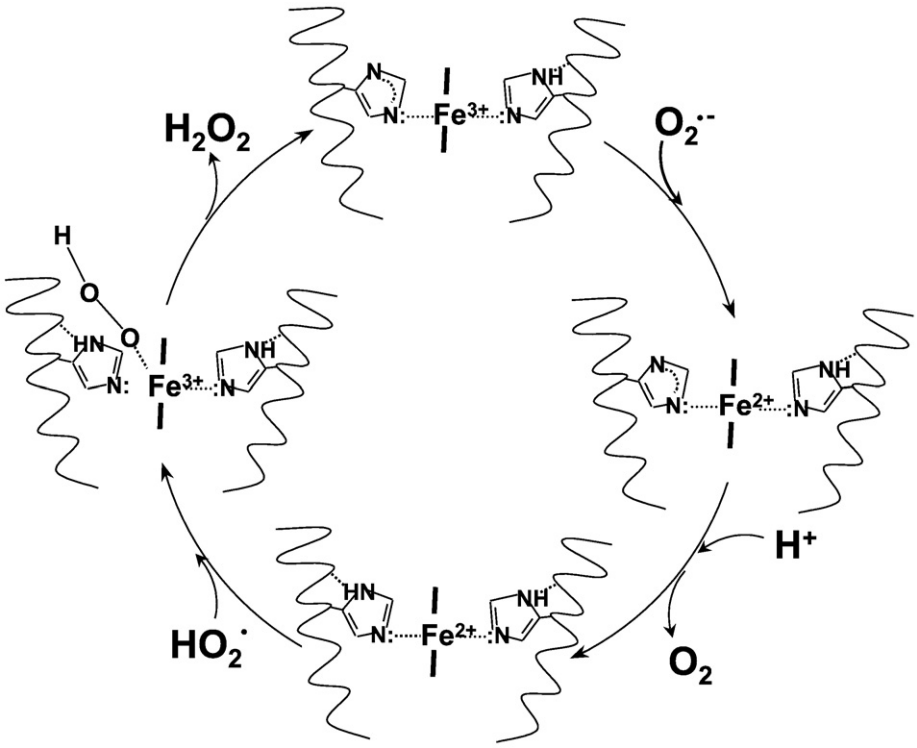

Scheme 1. Proposed model for the mechanisms of the involvement of ferric and ferrous heme iron intermediates in the SOO and the SOR activity of cyt b_{559}.

metal in superoxide-scavenger enzymes is able to both oxidize and reduce $O_2^{\cdot-}$ depending on the oxidation state of the metal and the protonation state of the nearby residues [38,57,58]. Here, it is proposed that the uprotonated IP form of cyt b_{559} serves as SOO that catalyze the one-electron oxidation of $O_2^{\cdot-}$ to O_2 (equation A). On the other hand, the protonated HP^{red} form of cyt b_{559} acts as SOR known to catalyze the one-electron reduction of $O_2^{\cdot-}$ to H_2O_2 (equation B). We suggest that these are redox state, redox potential and acid/base properties of cyt b_{559}, which modulate SOO and SOR activity of cyt b_{559}. Moreover, α-helix of cyt b_{559} is exposed to the exterior through a large cavity, which is present at the stromal surface of thylakoid membrane [8,59]. As the heme is exposed to this cavity, the interior of the cavity can have an influence on the redox state of cyt b_{559} [59]. Although the walls of this cavity are covered by hydrophobic groups, any change in the hydrophobic environment around the heme may cause it to become more accessible to solvent and favor low redox potential forms. These structural details strongly support the feasibility on the mechanism aspects of superoxide oxidation and reduction by HP^{red} and IP forms, respectively, as described in our study.

4.3.1. Superoxide oxidase activity of cyt b_{559}

Based on the fact that ferric heme iron has been proposed to be located near to the membrane edge in the less hydrophobic environment [13], the accessibility of $O_2^{\cdot-}$ to ferric heme iron is feasible. The negative charge carried by $O_2^{\cdot-}$ attracts it towards ferric heme iron, and results in reduction of the ferric heme iron by $O_2^{\cdot-}$. Due to the strong attraction forces between the ferric heme iron and electron cloud of nitrogen atom of the imidazole, it is proposed that the reduction of ferric heme iron by $O_2^{\cdot-}$ occurs as an outer-sphere reaction, which does not involve the direct binding of $O_2^{\cdot-}$ to the ferric heme iron. In accordance with this assumption, it has been recently demonstrated that oxidation of $O_2^{\cdot-}$ by transition metals process via an outer-sphere reaction pathway [60]. The fact that the ferric heme iron is located near to the membrane edge reveals that protons from the water phase are likely available for protonation of the imidazole group. Furthermore, the reduction of the ferric heme iron increased the electrostatic strength of N1–H bond and thus enhanced the affinity for the protons. Protonation of the N1 atom of imidazole ring makes environment around the heme more hydrophobic and results in the formation of hydrogen bond between imidazole N1–H group and the peptide backbone in the α-helix. In accordance with this proposal, it has been shown that the formation of hydrogen bond caused a structural change that increases the hydrophobicity around the heme and stabilizes the ferrous heme iron [15].

4.3.2. Superoxide reductase activity of cyt b_{559}

Based on the fact that ferrous heme iron is incorporated more deep in the membrane in a more hydrophobic environment [13], it is likely that the ferrous heme iron interacts with $HO_2^{\cdot}$ that could penetrate more easily inside the hydrophobic domain of the membrane. Due to the fact that $HO_2^{\cdot}$ is a neutral radical, the lack of the charge facilitates $HO_2^{\cdot}$ to penetrate to the ferrous heme iron and maintain its oxidation to the ferric heme iron. It is proposed that the ferrous heme iron generates less attraction force and weaker interaction with histidine ligand due to its less positive charge thereby causing shift of the electron cloud of nitrogen away from the ferrous heme iron. In such a case, it seems favorable that the interaction of hydroperoxyl radical with ferrous heme iron process via an inner-sphere reaction pathway. In accordance with this proposal, the reduction of superoxide by ferrous iron was suggested to proceed via the inner-sphere mechanism [61]. Based on the analogy with SOR, the inner-sphere electron transfer from the ferrous heme iron to hydroperoxyl radical is proposed to result in formation of the ferric-hydroperoxo intermediate (Scheme I) [62–64]. Because ferrous heme iron is incorporated deeper into the hydrophobic domain of membrane, the delivery of protons to redox active site is limited. It is proposed that oxidation of ferrous to ferric heme iron decreased the electrostatic strength of N1–H bond and thus lowered the affinity for the protons. It seems reasonable that deprotonation of the N1–H of histidine may also provide a second proton to proximal oxygen of ferric-hydroperoxo intermediate during the formation of H_2O_2. Previously, formation of

H_2O_2 was also demonstrated as one of the major pathways of ferric-hydroperoxo species, formed in another *b*-type of cytochrome, cyt *P450* [65]. The protonation of proximal oxygen immediately results in the cleavage of heme-oxygen bridge. Thus, dissociation of H_2O_2 as a product is followed by restoration of the sixth coordination of ferric iron with nitrogen of imidazole ring. Recently, it has been suggested for SOR enzymatic cycle that the proximal oxygen coordinated to ferric iron is replaced by axial glutamate (Glu^{47}) residue with liberation of H_2O_2 [66].

4.4. Physiological relevance

Three dimensional structure of PSII from thermophilic cyanobacteria showed that cofactors on the electron acceptor side of PSII are far away from the heme iron to sufficiently maintain a direct electron transfer reaction (heme iron is located approximately 50 Å and 30 Å from pheophytins of D1 and D2 proteins, respectively; it is 50 Å and 30 Å away from primary quinone acceptor (Q_A) and secondary quinone acceptor (Q_B) binding sites, respectively) [7,8]. Based on the results presented in this study, it seems likely that $O_2^{\cdot -}$ as a dangerous secondary by-product coming from inadequate PSII might sufficiently fulfill the function of an electron transport carrier between these cofactors and heme iron. Light-induced formation of $O_2^{\cdot -}$ on PSII electron acceptor side provides an alternative way for electron transport between these cofactors and heme iron of cyt b_{559} and thus might prevent over reduction of PSII electron acceptor side. The light-induced transformation between redox potential forms of cyt b_{559} has not been reported in control PSII membranes yet; however, the present model has demonstrated the SOO and the SOR function of cyt b_{559} based on the light-induced transformation between redox potential forms of cyt b_{559} in donor side inhibited PSII complex which are more often present in natural environment during photoinhibitory conditions.

Acknowledgements

This work was supported by the grants of The Ministry of Education, Youth and Sports of the Czech Republic MSM 6198959215. We are grateful to Dr. Dušan Lazár for data fitting. We thank Dr. Jan Hrbáč and Prof. Jan Lasovský for support with respect to the EPR measurements. We are grateful to unknown reviewers for their valuable comments and constructive criticism for the improvement of our manuscript.

References

[1] J. Whitmarsh, H.B. Pakrasi, Form and function of cytochrome *b*-559, in: D.R. Ort, C. Yocum (Eds.), Oxygenic Photosynthesis: The Light Reactions, Kluwer Academic Publishers, Dordrecht, The Netherlands, 1996, pp. 249–264.
[2] D.H. Stewart, G.W. Brudvig, Cytochrome *b*559 of photosystem II, Biochim. Biophys. Acta 1367 (1998) 63–87.
[3] G.T. Babcock, W.R. Widger, W.A. Cramer, W.A. Oertling, J.G. Metz, Axial ligands of chloroplast cytochrome *b*-559 — identification and requirement for a haem-cross-linked polypeptide structure, Biochemistry 24 (1985) 3638–3645.
[4] G.S. Tae, M.T. Black, W.A. Cramer, O. Vallon, L. Bogorad, Thylakoid membrane protein topography: transmembrane orientation of the chloroplast cytochrome *b*-559 psbE gene product, Biochemistry 27 (1988) 9075–9080.
[5] A. Zouni, H.T. Witt, J. Kern, P. Fromme, N. Krauss, W. Saenger, P. Orth, Crystal structure of photosystem II from *Synechococcus elongatus* at 3.8 A resolution, Nature 409 (2001) 739–743.
[6] N. Kamiya, J.R. Shen, Crystal Structure of oxygen-evolving photosystem II from *Thermosynechococcus vulcanus* at 3.7 Å resolution, Proc. Natl. Acad. Sci. U.S.A. 100 (2003) 98–103.
[7] K.N. Ferreira, T.M. Iverson, K. Maghlaoui, J. Barber, S. Iwata, Architecture of the photosynthetic oxygen-evolving center, Science 303 (2004) 1831–1838.
[8] B. Loll, J. Kern, W. Saenger, A. Zouni, J. Biesiadka, Towards complete cofactor arrangement in the 3.0 A resolution structure of photosystem II, Nature 438 (2005) 1040–1044.
[9] G.S. Tae, W.A. Cramer, Topography of the heme prosthetic group of cytochrome *b*559 in photosystem II reaction center, Biochemistry 33 (1994) 10060–10068.
[10] L.K. Thompson, A.F. Miller, C.A. Buser, J.C. De Paula, G.W. Brudwig, Characterization of the multiple forms of cytochrome *b*559 in photosystem II, Biochemistry 28 (1989) 8048–8056.
[11] O. Kaminskaya, J. Kurreck, K.D. Irrgang, G. Renger, V. Shuvalov, Redox and spectral properties of cytochrome *b*559 in different preparations of photosystem II, Biochemistry 38 (1999) 16223–16235.
[12] N. Mizusawa, T. Yamashita, M. Miyao, Restoration of the high-potential form of cytochrome *b*559 of photosystem II occurs via a two-step mechanism under illumination in the presence of manganese ions, Biochim. Biophys. Acta 1410 (1999) 273–286.
[13] L.I. Krishtalik, G.S. Tae, D.A. Cherepanov, W.A. Cramer, The redox properties of cytochromes *b* imposed by the membrane electrostatic environment, Biophys. J. 65 (1993) 184–195.
[14] C. Berthomieu, A. Boussac, W. Mantele, J. Breton, E. Nabedryk, Molecular changes following oxidoreduction of cytochrome *b*559 characterized by Fourier transform infrared different spectroscopy and electron paramagnetic resonance: photooxidation in photosystem II and electrochemistry of isolated cytochrome *b*559 and iron protoporphyrin IX-bisimidazole model compounds, Biochemistry 31 (1992) 11460–11471.
[15] M. Roncel, J.M. Ortega, M. Losada, Factors determining the special redox properties of photosynthetic cytochrome *b*559, Eur. J. Biochem 268 (2001) 4961–4968.
[16] J.M. Ortega, M. Hervás, M.A. De la Rosa, M. Losada, pH-dependent photoreactions of the high- and low-potential forms of cytochrome *b*559 in spinach PSII-enriched membranes, Photosynth. Res. 46 (1995) 185–191.
[17] O. Kaminskaya, V. Shuvalov, G. Renger, Two reaction pathways for transformation of high potential cytochrome *b*559 of PS II into the intermediate potential form, Biochim. Biophys. Acta 1767 (2007) 550–558.
[18] O. Kaminskaya, V. Shuvalov, G. Renger, Evidence for a novel quinone binding site in the photosystem II complex that regulates the redox potential of cytochrome *b*559, Biochemistry, Biochemistry 46 (2007) 1091–1105.
[19] A.W. Rutherford, J.L. Zimmermann, P. Mathis, The effect of herbicides on components of the PS II reaction centre measured by EPR, FEBS Lett. 165 (1984) 156–162.
[20] A. Tiwari, A. Jajoo, S. Bharti, Heat-induced changes in the EPR signal of tyrosine D (Y_D^{ox}): a possible role of cytochrome *b*559, J. Bioenerg. Biomembr. 40 (2008) 237–243.
[21] H. Matsuda, W.L. Butler, Restoration of high-potential cytochrome *b*559 in liposomes, Biochim. Biophys. Acta 725 (1983) 320–324.
[22] R. Gadjieva, F. Mamedov, G. Renger, S. Styring, Interconversion of low- and high-potential forms of cytochrome *b*559 in tris-washed photosystem II membranes under aerobic and anaerobic conditions, Biochemistry 38 (1999) 10578–10589.
[23] F. Mamedov, R. Gadjieva, R. Styring, Oxygen-induced changes in the redox state of the cytochrome b_{559} in photosystem II depend on the integrity of the Mn cluster, Physiol. Plant. 131 (2007) 41–49.
[24] B. Ke, The primary electron donor of photosystem II, p680, and photoinhibition, in: B. Ke (Ed.), Photosynthesis: Photobiochemistry and Photobiophysics, Kluwer Academic Publishers, Dordrecht, The Netherlands, 2001, pp. 271–288.
[25] L. Nedbal, G. Samson, J. Whitmarsh, Redox state of one electron component controls the rate of photoinhibition of photosystem II, Proc. Natl. Acad. Sci. U.S.A. 89 (1992) 7923–7929.
[26] J. Barber, J. De Las Rivas, A functional model for the role of cytochrome *b*559 in the protection against donor and acceptor side photoinhibition, Proc. Natl. Acad. Sci. U.S.A. 90 (1993) 10942–10946.
[27] M. Poulson, G. Samson, J. Whitmarsh, Evidence that cytochrome *b*559 protects photosystem II against photoinhibition, Biochemistry 34 (1995) 10932–10938.
[28] J. Kruk, K. Strzalka, Redox changes of cytochrome b_{559} in the presence of plastoquinones, J. Biol. Chem. 276 (2001) 86–91.
[29] P. Pospíšil, I. Šnyrychová, J. Kruk, K. Strzałka, J. Nauš, Evidence that cytochrome b_{559} is involved in superoxide production in photosystem II: effect of synthetic short-chain plastoquinones in a cytochrome b_{559} tobacco mutant, Biochem. J. 397 (2006) 321–327.
[30] J. Hanley, Y. Deligiannakis, A. Pascal, P. Faller, A.W. Rutherford, Carotenoid oxidation in photosystem II, Biochemistry 38 (1999) 8189–8195.
[31] P. Faller, R.J. Debus, K. Brettel, M. Sugiura, A.W. Rutherford, A. Boussac, Rapid formation of the stable tyrosyl radical in photosystem II, Proc. Natl. Acad. Sci. U.S.A. 98 (2001) 14368–14373.
[32] P. Faller, C. Fufezan, A.W. Rutherford, Side-path electron donors: cytochrome b_{559}, chlorophyll Z and β-carotene, in: T. Wydrzynski, K. Satoh (Eds.), Photosystem II: The Light-driven Water: Plastoquinone Oxidoreductase, Springer Publishers, Dordrecht, The Netherlands, 2005, pp. 347–365.
[33] J. Kruk, K. Strzalka, Dark reoxidation of the plastoquinone-pool is mediated by the low-potential form of cytochrome *b*-559 in spinach thylakoids, Photosynth. Res. 62 (1999) 273–279.
[34] N. Bondarava, L. De Pascalis, S. Al-Babili, C. Goussias, J.R. Golecki, P. Beyer, R. Bock, A. Krieger-Liszkay, Evidence that cytochrome *b*559 mediates the oxidation of reduced plastoquinone in the dark, J. Biol. Chem. 278 (2003) 13554–13560.
[35] G.M. Ananyev, G. Renger, U. Wacker, V. Klimov, The Photoproduction of superoxide radicals and the superoxide-dismutase activity of photosystem II. The possible involvement of cytochrome *b*559, Photosynth. Res. 41 (1994) 327–338.
[36] F.E. Jenney, M.F.J.M. Verhagen, X. Cui, M.W.W. Adams, Anaerobic microbes: oxygen detoxification without superoxide dismutase, Science 286 (1999) 306–309.
[37] M. Lombard, M. Fontecave, D. Touati, V. Nivière, Reaction of the desulfoferrodoxin from *Desulfoarculus baarsii* with superoxide anion. Evidence for a superoxide reductase activity, J. Biol. Chem. 275 (2000) 115–121.
[38] M.W.W. Adams, F.E. Jenney, M.D. Clay, M.K. Johnson, Superoxide reductase: fact or fiction, J. Biol. Inorg. Chem. 7 (2002) 647–652.
[39] A.P. Yeh, Y. Hu, F.E. Jenney, M.W.W. Adams, D.C. Rees, Structures of the superoxide reductase from *Pyrococcus furiosus* in the oxidized and reduced states, Biochemistry 39 (2000) 2499–2508.

[40] M.D. Clay, C.A. Cosper, F.E. Jenney Jr., M.W.W. Adams, M.K. Johnson, Nitric oxide binding at the mononuclear active site of reduced *Pyrococcus furiosus* superoxide reductase, Proc. Natl. Acad. Sci. U.S.A. 100 (2003) 3796–3801.
[41] V. Adam, A. Royant, V. Nivière, F.P. Molina-Heredia, D. Bourgeois, Structure of superoxide reductase bound to ferrocyanide and active site expansion upon X-ray-induced photo-reduction, Structure (London) 12 (2004) 5032–5040.
[42] D.A. Berthold, G.T. Babcock, C.F. Yocum, A highly resolved, oxygen evolving photosystem II preparation from spinach thylakoid membranes, FEBS Lett. 134 (1981) 231–234.
[43] R.C. Ford, M.C.W. Evans, Isolation of a photosystem II preparation from higher plants with highly enriched oxygen evolution activity, FEBS Lett. 160 (1983) 159–164.
[44] L.X. Shi, S.J. Kim, A. Marchant, C. Robinson, W.P. Schröder, Characterization of the PsbX protein from Photosystem II and light regulation of its gene expression in higher plants, Plant Mol. Biol. 40 (1999) 737–744.
[45] U. Hegde, S. Padhye, L. Kovács, A. Vozárand, S. Demeter, Modification of histidine residues of photosystem II by diethylpyrocarbonate inhibits the electron transfer between the primary (Q_A) and secondary (Q_B) quinone acceptors, Z. Naturforsch. 48c (1993) 896–902.
[46] P.L. Dutton, Redox potentiometry: determination of midpoint potentials of oxidation–reduction components of biological electron-transfer system, Methods Enzymol. 54 (1978) 411–435.
[47] G. Olive, A. Mercier, F.L. Moigne, A. Rockenbauer, P. Tordo, 2-ethoxycarbonyl-2-methyl-3,4-dihydro-2H-pyrrole-1-oxide: evaluation of the spin trapping properties, Free Radical Biol. Med. 28 (2000) 403–408.
[48] H. Zhang, J. Joseph, J. Vasquez-Vivar, H. Karoui, C. Nsanzumuhire, P. Martasek, P. Tordo, B. Kalyanaraman, Detection of superoxide anion using an isotopically labeled nitrone spin trap: potential biological applications, FEBS Lett. 473 (2000) 58–62.
[49] J. De Las Rivas, J. Klein, J. Barber, pH sensitivity of the redox state of cytochrome *b*559 may regulate its function as a protectant against donor and acceptor side photoinhibition, Photosynth. Res. 46 (1995) 193–202.
[50] M. Tanokura, ^{1}H-NMR study on the tautomerism of the imidazole ring of histidine residues: I. Microscopic p*K* values and molar ratios of tautomers in histidine-containing peptides, Biochim. Biophys. Acta 742 (1983) 576–585.
[51] A. Azzi, R.P. Casey, M.J. Nalecz, The effect of *N*,*N*′-dicyclohexylcarbodiimide on enzymes of bioenergetic relevance, Biochim. Biophys. Acta 768 (1984) 209–226.
[52] P. Pospíšil, A. Arató, A. Krieger-Liszkay, A.W. Rutherford, Hydroxyl radical generation by photosystem II, Biochemistry 43 (2004) 6783–6792.
[53] P.M. Wood, The potential diagram for oxygen at pH 7, Biochem. J. 253 (1988) 287–289.
[54] J.A. Kovacs, How iron activates O_2, Science 299 (2003) 1024–1025.
[55] D.M. Kurtz, E.D. Coulter, The mechanism(s) of superoxide reduction by superoxide reductases in vitro and in vivo, J. Biol. Inorg. Chem. 7 (2002) 653–658.
[56] L.M. Brines, J.A. Kovacs, Understanding the mechanism of superoxide reductase (SOR), Eur. J. Inorg. Chem. 1 (2007) 29–38.
[57] S.I. Liochev, I. Fridovich, Copper- and zinc-containing superoxide dismutase can act as a superoxide reductase and a superoxide oxidase, J. Biol. Chem. 275 (2000) 38482–38485.
[58] F.P. Molina-Heredia, C. Houée-Levin, C. Berthomieu, D. Touati, E. Tremey, V. Favaudon, V. Adam, V. Nivière, Detoxification of superoxide without production of H_2O_2: antioxidant activity of superoxide reductase complexed with ferrocyanide, Proc. Natl. Acad. Sci. U.S.A. 103 (2006) 14750–14755.
[59] B. Loll, J. Kern, W. Saenger, A. Zouni, J. Biesiadka, Lipids in photosystem II: interactions with protein and cofactors, Biochim. Biophys. Acta 1767 (2007) 509–519.
[60] I. Weinstock, Outer-sphere oxidation of the superoxide radical anion, Inorg. Chem. 47 (2007) 404–406.
[61] D.M. Kurtz, Avoiding high-valent iron intermediates: superoxide reductase and rubrerythrin, J. Inorg. Biochem. 100 (2006) 679–693.
[62] M. Lombard, C. Houee-Levin, D. Touati, M. Fontecave, V. Nivière, Superoxide reductase from *Desulfoarculus baarsii*: reaction mechanism and role of glutamate 47 and lysine 48 in catalysis, Biochemistry 40 (2001) 5032–5040.
[63] J.P. Emerson, E.D. Coulter, R.S. Phillips, D.M. Kurtz, Kinetics of the superoxide reductase catalytic cycle, J. Biol. Chem. 278 (2003) 39662–39668.
[64] C. Mathé, T.A. Mattioli, O. Horner, M. Lombard, J.M. Latour, M. Fontecave, V. Niviére, Identification of iron(III) peroxo species in the active site of the superoxide reductase SOR from *Desulfoarculus baarsii*, J. Am. Chem. Soc. 124 (2002) 4966–4967.
[65] G. Denisov, T.M. Makris, S.G. Sliger, I. Schlichting, Structure and chemistry of cytochrome *P450*, Chem. Rev. 105 (2005) 2253–2277.
[66] G. Katona, P. Carpentier, V. Nivière, P. Amara, V. Adam, J. Ohana, N. Tsanov, D. Bourgeois, Raman spectroscopy confirmed the entrapment of iron(III)-peroxo intermediates in superoxide reductase crystals, which displayed different conformations/interactions within the crystallographic asymmetric unit, Science 316 (2007) 449–453.